Noname manuscript No.
(will be inserted by the editor)

Shape Optimization of Flow Field Improving Hydrodynamic Stability

Takashi Nakazawa · Hideyuki Azegami

Received: date / Accepted: date

Abstract This paper presents a solution of a shape optimization problem of a flow field for delaying transition from a laminar flow to a turbulent flow. Mapping from an initial domain to a new domain is chosen as the design variable. Main problems are defined by the stationary Navier–Stokes problem and an eigenvalue problem assuming a linear disturbance on the solution of the stationary Navier–Stokes problem. The maximum value of the real part of the eigenvalue is used as an objective cost function. The shape derivative of the cost function is defined as the Fréchet derivative of the cost function with respect to arbitrary variation of the design variable, which denotes the domain variation, and is evaluated using the Lagrange multiplier method. To obtain a numerical solution, we use an iterative algorithm based on the H^1 gradient method using the finite element method. To confirm the validity of the solution, a numerical example for two-dimensional Poiseuille flow with a sudden expansion is presented. Results reveal that a critical Reynolds number increases by the iteration of reshaping.

Keywords Shape optimization · Fluid dynamics · Hydrodynamic stability

Mathematics Subject Classification (2000) 65K10 · 65N25

T. Nakazawa
Graduate School of Information Science, Tohoku University, Japan, Aoba-ku, Aramaki Aza, Aoba 6-3, Sendai-shi, Miyagi-ken, 980-8579
E-mail: nakazawa@math.is.tohoku.ac.jp

H. Azegami
Graduate School of Information Science, Nagoya University, Japan, Chikusa-ku Hurou-chou, Nagiya-shi, Aichi-ken, 464-8601
E-mail: azegami@is.nagoya-u.ac.jp

1 Introduction

Flow control to delay transition from a laminar flow to turbulent flow is a key technology used in the design of fluid-related machinery such as airplanes and turbines. In techniques to delay the transition, active control and passive control have been used. In active control, external forces in feedback systems are chosen as design variables [7,8,30]. In passive control, positions of actuators and sensors are chosen as design variables [11,22]. However, as far as we know, no technique choosing geometrical shape of the flow field as a design variable in nonparametric formulation has been reported. In this study, we emphasize examination of the optimization problem of the geometrical shape of the flow field increasing the critical Reynolds number for the transition.

For shape optimization problems in a flow field, a theoretical framework of shape derivatives, which is defined as the Fréchet derivative with respect to arbitrary domain variation for stationary Stokes and Navier–Stokes problems, has been investigated since the 1970s [15,19,24–27]. The framework is based on general theories of shape derivatives [9,13,14,31]. For the cost function, dissipation energy was used mainly. Numerous numerical analyses of stationary problems have been conducted [12,16,17,28]. However, direct application of the gradient method using the numerical result of the shape derivative of cost function often results in oscillating shapes in engineering fields [18].

To avoid oscillation, a method using the Laplace operator to recover the lack of smoothness of the shape derivative was proposed. It was called the traction method in early years [1,5,6]. As a similar method, designated as the H^1 gradient method, for a topological optimization problem of the density type [4], we refer to the traction method as the H^1 gradient method for the shape optimization problem. The precise definition and basic properties of the H^1 gradient method for shape optimization problem are presented in [2,3]. This reshaping method has also been applied to shape optimization problems in flow fields [20,21]. In these studies, however, dissipation energy was used as the cost function.

Based on the background, the main contributions of this work are to construct a shape optimization problem of a flow field increasing the critical Reynolds number for the transition and to show its solution. To define the cost function, we use two main problems of the stationary Navier–Stokes problem and an eigenvalue problem assuming a linear disturbance on the solution of the stationary Navier–Stokes problem. Using the solution of the eigenvalue problem, we chose the maximum value of the real part of the eigenvalues as the cost function. The shape derivative of the cost function is evaluated by using the Lagrange multiplier method. For a reshaping scheme, the H^1 gradient method is employed.

To confirm the validity of choosing the cost function and the evaluation method of its shape derivative, two-dimensional Poiseuille flow with a sudden expansion is selected as the main problem of the stationary Navier–Stokes problem because the critical Reynolds number $\mathrm{Re_c}$ has been investigated [23,

29]. In this paper, $\mathrm{Re_c} = 40.24$ reported by Mizushima and Shiotani [23] is used as a reference value before optimization.

This paper is organized in the following way. In Section 2, after defining an initial domain and mapping from the initial domain to a new domain as a design variable, we define the cost function using the solutions of two main problems, and formulate the shape optimization problem. In Subsection 2.2, a formula of the shape derivative of the domain integral is presented for later use. Using the formula, the evaluation method of the cost function is shown in Section 3. The numerical scheme by the finite element method using the H^1 gradient method for reshaping is shown in Section 4. Finally, in Section 5, the numerical results for the two-dimensional Poiseuille flow with a sudden expansion obtained using the present approach are presented.

2 Problem formulation

Considering that numerical results will be presented for the two-dimensional Poiseuille flow with a sudden expansion, we define an initial domain and domain variations in the following way.

2.1 Initial domain

Using the two-dimensional Cartesian coordinate system, a point is denoted as $\boldsymbol{x} = (x, y) \in \mathbb{R}^2$. We define an initial domain as

$$\Omega_0 = \left\{(x, y) \in \mathbb{R}^2 \mid ([0, 6] \times [-1, 1]) \cup ([6, 42] \times [-3, 3])\right\},$$

inflow and outflow boundaries as

$$\begin{aligned} \Gamma_{\mathrm{in}\,0} &= \left\{(x, y) \in \mathbb{R}^2 \mid x = 0,\ -1 \le y \le 1\right\}, \\ \Gamma_{\mathrm{out}\,0} &= \left\{(x, y) \in \mathbb{R}^2 \mid x = 42,\ -3 \le y \le 3\right\}, \end{aligned}$$

and wall boundary of the initial domain as $\Gamma_{\mathrm{wall}\,0} = \partial\Omega_0 \setminus (\bar{\Gamma}_{\mathrm{in}\,0} \cup \bar{\Gamma}_{\mathrm{out}\,0})$, where $\bar{(\cdot)}$ denotes the closure. In this paper, we assume that $\Gamma_{\mathrm{wall}\,0}$ is variable.

2.2 Domain variation

Using the initial domain, we define the domain variation in the following way. Let $\boldsymbol{i} + \boldsymbol{\phi} : \mathbb{R}^2 \to \mathbb{R}^2$ be a bi-Lipschitz transform and D be the set of $\boldsymbol{\phi}$, where $\boldsymbol{i}$ denotes identity mapping. For a $\boldsymbol{\phi} \in D$, let a varied domain $\Omega(\boldsymbol{\phi})$ and boundary $\Gamma_{\mathrm{wall}}(\boldsymbol{\phi})$ be defined respectively as $(\boldsymbol{i} + \boldsymbol{\phi})(\Omega_0)$ and $(\boldsymbol{i} + \boldsymbol{\phi})(\Gamma_{\mathrm{wall}\,0})$. To define the Fréchet derivative with respect to arbitrary domain variation, we define

$$X = \left\{\boldsymbol{\psi} \in H^1(\mathbb{R}^2; \mathbb{R}^2) \mid \boldsymbol{\psi} = \boldsymbol{0} \text{ on } \Gamma_{\mathrm{in}\,0} \cup \Gamma_{\mathrm{out}\,0}\right\} \tag{1}$$

as the function space for domain variation.

For $\boldsymbol{\phi} \in D$, let ζ be a real-valued function of $\varphi \in C^1\left(D; H^2\left(\mathbb{R}^2; \mathbb{R}\right)\right)$ and $\nabla\varphi(\boldsymbol{\phi})$, and

$$L(\boldsymbol{\phi}) = \int_{\Omega(\boldsymbol{\phi})} \zeta(\varphi(\boldsymbol{\phi}), \nabla\varphi(\boldsymbol{\phi}))dx.$$

The shape derivative $L'[\boldsymbol{\psi}]$ of L is given for all $\boldsymbol{\psi} \in X$ as

$$L'[\boldsymbol{\psi}] = \int_{\Omega(\boldsymbol{\phi})} \zeta'[\boldsymbol{\psi}]dx + \int_{\Gamma(\boldsymbol{\phi})} \zeta\boldsymbol{\nu} \cdot \boldsymbol{\psi} d\gamma, \tag{2}$$

where $\zeta'[\boldsymbol{\psi}] = \zeta_\varphi[\varphi'[\boldsymbol{\psi}]] + \zeta_{\nabla\varphi}[\nabla\varphi'[\boldsymbol{\psi}]]$ denotes the shape derivative of ζ and $\boldsymbol{\nu}$ denotes the outward unit normal vector on the boundary ([2] Proposition (4.9), p.101).

2.3 Main problems

We define the main problems for shape optimization problem increasing stability. We assume that $\boldsymbol{\phi} \in D$ is given, that is $\Omega(\boldsymbol{\phi})$ and $\Gamma_{\rm wall}(\boldsymbol{\phi})$ are determined, and that the prescribed fluid velocity is given as $\hat{\boldsymbol{u}}_{\rm D} = (\hat{u}_{\rm D}, \hat{v}_{\rm D}) \in \left\{\hat{\boldsymbol{u}} \in H^1\left(\mathbb{R}^2, \mathbb{R}^2\right) \mid \boldsymbol{\nabla} \cdot \hat{\boldsymbol{u}} = 0,\ \hat{\boldsymbol{u}} = \boldsymbol{0} \text{ on } \Gamma_{\rm wall}(\boldsymbol{\phi})\right\}$. Using the definitions, we define the stationary Navier–Stokes problem as described below. Let Re denote the Reynolds number.

Problem 1 (Stationary Navier-Stokes) For $\boldsymbol{\phi} \in D$, find $(\hat{\boldsymbol{u}}, \hat{p}) : \Omega(\boldsymbol{\phi}) \to \mathbb{R}^3$ such that

$$(\hat{\boldsymbol{u}} \cdot \nabla)\,\hat{\boldsymbol{u}} = -\nabla\hat{p} + \frac{1}{\rm Re}\triangle\hat{\boldsymbol{u}} \quad \text{in } \Omega(\boldsymbol{\phi}), \tag{3}$$

$$\nabla \cdot \hat{\boldsymbol{u}} = 0 \quad \text{in } \Omega(\boldsymbol{\phi}), \tag{4}$$

$$\frac{1}{\rm Re}(\boldsymbol{\nabla}\hat{\boldsymbol{u}}^{\rm T})\boldsymbol{\nu} - \hat{p}\boldsymbol{\nu} = \boldsymbol{0} \quad \text{on } \Gamma_{\rm out\,0}, \tag{5}$$

$$\hat{\boldsymbol{u}} = \hat{\boldsymbol{u}}_{\rm D} \text{ on } \Gamma_{\rm in\,0}, \tag{6}$$

$$\hat{\boldsymbol{u}} = \boldsymbol{0} \text{ on } \Gamma_{\rm wall}(\boldsymbol{\phi}). \tag{7}$$

Weak forms of Problem 1 are written in the following way. Let

$$U = \left\{\hat{\boldsymbol{u}} \in H^1(\Omega(\boldsymbol{\phi}); \mathbb{R}^2) |\ \hat{\boldsymbol{u}} = \hat{\boldsymbol{u}}_{\rm D} \text{ on } \Gamma_{\rm in\,0} \cup \Gamma_{\rm wall}(\boldsymbol{\phi})\right\},$$
$$Q = L^2(\Omega(\boldsymbol{\phi}); \mathbb{R})$$

respectively represent the sets of velocity $\hat{\boldsymbol{u}}$ and pressure $\hat{p}$, and

$$W = \left\{\hat{\boldsymbol{w}} \in H^1(\Omega(\boldsymbol{\phi}); \mathbb{R}^2) |\ \hat{\boldsymbol{w}} = \boldsymbol{0} \text{ on } \Gamma_{\rm in\,0} \cup \Gamma_{\rm wall}(\boldsymbol{\phi})\right\}$$

be the set of trial functions $\hat{\boldsymbol{w}}$ for velocity. The weak forms of Problem 1 are written as $(\hat{\boldsymbol{u}}, \hat{p}) \in U \times Q$ such that

$$\int_{\Omega(\boldsymbol{\phi})} \left\{((\hat{\boldsymbol{u}} \cdot \nabla)\,\hat{\boldsymbol{u}}) \cdot \hat{\boldsymbol{w}} - \hat{p}\nabla \cdot \hat{\boldsymbol{w}} + \frac{1}{\rm Re}(\nabla\hat{\boldsymbol{u}}^{\rm T}) \cdot (\nabla\hat{\boldsymbol{w}}^{\rm T})\right\} dx = 0, \tag{8}$$

$$-\int_{\Omega(\boldsymbol{\phi})} \hat{q}\nabla\cdot\hat{\boldsymbol{u}}dx = 0 \tag{9}$$

for all $(\hat{\boldsymbol{w}}, \hat{q}) \in W \times Q$.

Using the solution of Problem 1, we define the linear disturbance problem in the following way. Using $\epsilon > 0$ as a parameter for magnitude of disturbance, we assume the velocity and pressure including a linear disturbance $(\bar{\boldsymbol{u}}, \bar{p})$ as

$$\boldsymbol{u} = \hat{\boldsymbol{u}} + \epsilon\bar{\boldsymbol{u}} + O(\epsilon^2), \tag{10}$$
$$p = \hat{p} + \epsilon\bar{p} + O(\epsilon^2), \tag{11}$$

where $(\hat{\boldsymbol{u}}, \hat{p})$ are the solutions of Problem 1. Substituting (10) and (11) into the nonstationary Navier–Stokes equations and the continuity equation, subtracting equations (3) and (4), and neglecting the nonlinear terms with respect to ϵ, linear disturbance equations are obtained as

$$\frac{\partial\bar{\boldsymbol{u}}}{\partial t} + N(\bar{\boldsymbol{u}}, \hat{\boldsymbol{u}}) = -\nabla\bar{p} + \frac{1}{\mathrm{Re}}\triangle\bar{\boldsymbol{u}} \quad \text{in } \Omega(\boldsymbol{\phi}), \tag{12}$$
$$\nabla\cdot\bar{\boldsymbol{u}} = 0 \quad \text{in } \Omega(\boldsymbol{\phi}), \tag{13}$$

where $N(\,\cdot\,,\,\cdot\,)$ is a bilinear form defined for $\boldsymbol{f}, \boldsymbol{g} \in U$ as

$$N(\boldsymbol{f}, \boldsymbol{g}) = (\boldsymbol{f}\cdot\nabla)\,\boldsymbol{g} + (\boldsymbol{g}\cdot\nabla)\,\boldsymbol{f}.$$

Following the standard formulation for the linear stability analysis, we assume

$$\bar{\boldsymbol{u}}(t) = \tilde{\boldsymbol{u}}e^{\lambda t} + \left(\tilde{\boldsymbol{u}}e^{\lambda t}\right)^{\mathrm{c}}, \tag{14}$$
$$\bar{p}(t) = \tilde{p}e^{\lambda t} + \left(\tilde{p}e^{\lambda t}\right)^{\mathrm{c}}, \tag{15}$$

where $\lambda \in \mathbb{C}$ and $(\tilde{\boldsymbol{u}}, \tilde{p}) \in \tilde{U} \times \tilde{Q}$ respectively denote the complex linear growth rate and the complex velocity and pressure modes and

$$\tilde{U} = \left\{\tilde{\boldsymbol{u}} \in H^1(\Omega(\boldsymbol{\phi}); \mathbb{C}^2) |\ \tilde{\boldsymbol{u}} = \boldsymbol{0} \text{ on } \Gamma_{\mathrm{wall}}(\boldsymbol{\phi}) \cup \Gamma_{\mathrm{in}\,0}\right\},$$
$$\tilde{Q} = L^2(\Omega(\boldsymbol{\phi}); \mathbb{C}).$$

Here, $(\,\cdot\,)^{\mathrm{c}}$ represents the complex conjugate.

Here, substituting (14) and (15) into (12) and (13), one obtains an eigenvalue problem for the linear disturbance in the following way.

Problem 2 (Linear disturbance) Let $\boldsymbol{\phi} \in D$ and the solution $(\hat{\boldsymbol{u}}, \hat{p}) \in U \times Q$ of Problem 1 be given. Find $\lambda_i \in \mathbb{C}$ and $(\tilde{\boldsymbol{u}}_i, \tilde{p}_i) : \Omega(\boldsymbol{\phi}) \to \mathbb{C}^3$ for $i \in \{1, 2, \cdots\}$ such that

$$\lambda_i\tilde{\boldsymbol{u}}_i + N(\tilde{\boldsymbol{u}}_i, \hat{\boldsymbol{u}}) = -\nabla\tilde{p}_i + \frac{1}{\mathrm{Re}}\triangle\tilde{\boldsymbol{u}}_i \quad \text{in } \Omega(\boldsymbol{\phi}), \tag{16}$$
$$\nabla\cdot\tilde{\boldsymbol{u}}_i = 0 \quad \text{in } \Omega(\boldsymbol{\phi}), \tag{17}$$
$$\frac{1}{\mathrm{Re}}(\boldsymbol{\nabla}\tilde{\boldsymbol{u}}_i^{\mathrm{T}})\boldsymbol{\nu} - \tilde{p}_i\boldsymbol{\nu} = \boldsymbol{0} \quad \text{on } \Gamma_{\mathrm{out}\,0}, \tag{18}$$
$$\tilde{\boldsymbol{u}} = \boldsymbol{0} \quad \text{on } \Gamma_{\mathrm{in}\,0} \cup \Gamma_{\mathrm{wall}}(\boldsymbol{\phi}). \tag{19}$$

The stability of the steady state flow is evaluated with Real$[\lambda_i]$ for $i \in \{1, 2, \cdots\}$. If Real$[\lambda_i] < 0$ for all $r \in \{1, 2, \cdots\}$, then the solution $(\hat{\boldsymbol{u}}, \hat{p}) \in U \times Q$ of Problem 1 is evaluated as a stable flow. Otherwise, in the case of Real$[\lambda_i] \geq 0$ for some $r \in \{1, 2, \cdots\}$, the $(\hat{\boldsymbol{u}}, \hat{p})$ is evaluated as an unstable flow. Therefore, the maximum value of the real part of the eigenvalue becomes an indicator of the flow stability.

Weak forms of Problem 2 are written as finding λ_i and $(\tilde{\boldsymbol{u}}_i, \tilde{p}_i) \in \tilde{U} \times \tilde{Q}$ for $i \in \{1, 2, \cdots\}$ such that

$$\int_{\Omega(\boldsymbol{\phi})} \left\{ \lambda_i \tilde{\boldsymbol{u}}_i \cdot \tilde{\boldsymbol{w}}^{\mathrm{c}} + N(\tilde{\boldsymbol{u}}_i, \hat{\boldsymbol{u}}) \cdot \tilde{\boldsymbol{w}}^{\mathrm{c}} - \tilde{p}_i \nabla \cdot \tilde{\boldsymbol{w}}^{\mathrm{c}} + \frac{1}{\mathrm{Re}} (\nabla \tilde{\boldsymbol{u}}_i^{\mathrm{T}}) \cdot (\nabla \tilde{\boldsymbol{w}}^{\mathrm{cT}}) \right\} dx = 0, \tag{20}$$

$$- \int_{\Omega(\boldsymbol{\phi})} \tilde{q}^{\mathrm{c}} \nabla \cdot \tilde{\boldsymbol{u}}_i dx = 0 \tag{21}$$

for all $(\tilde{\boldsymbol{w}}, \tilde{q}) \in \tilde{U} \times \tilde{Q}$.

2.4 Shape optimization problem

Using the solutions of the two main problems, let us define a cost function for a shape optimization problem. Considering that the maximum value of the real part of the eigenvalues becomes an indicator of the flow stability, we define a cost function of the shape optimization problem using the solution of Problem 2 as

$$f(\lambda_r) = 2\mathrm{Real}[\lambda_r] = \lambda_r + \lambda_r^{\mathrm{c}} \tag{22}$$

where r is the mode number such that Real$[\lambda_i]$ is the maximum for every mode numbers i. Assuming that there exists such r in Problem 2, we define a shape optimization problem in the following way.

Problem 3 (Shape optimization) Let f be defined as (22). Find $\Omega(\boldsymbol{\phi})$ such that

$$\min_{\boldsymbol{\phi} \in D} \big\{ f(\lambda_r) \;\big|\; (\hat{\boldsymbol{u}}, \hat{p}) \in U \times Q, \text{ Problem 1}, \\ (\lambda_r, \tilde{\boldsymbol{u}}_r, \tilde{p}_r) \in \mathbb{C} \times \tilde{U} \times \tilde{Q}, \text{ Problem 2} \big\}.$$

3 Evaluation of the shape derivative of the cost function

To solve Problem 3, we use the algorithm with the H^1 gradient method. To use the method, the shape derivative $f'[\boldsymbol{\psi}]$ of the cost function f is required. In this paper, we derive the equations to evaluate $f'[\boldsymbol{\psi}]$ using the Lagrange multiplier method.

We put the Lagrange function L as

$$
\begin{aligned}
&L(\boldsymbol{\phi}, \hat{\boldsymbol{u}}, \hat{p}, \hat{\boldsymbol{w}}, \hat{q}, \lambda_r, \tilde{\boldsymbol{u}}_r, \tilde{p}_r, \tilde{\boldsymbol{w}}, \tilde{q}) = \\
&\quad 2\mathrm{Real}[\lambda_r] \\
&\quad - \int_{\Omega(\boldsymbol{\phi})} \left\{ \left((\hat{\boldsymbol{u}} \cdot \nabla)\, \hat{\boldsymbol{u}} \right) \cdot \hat{\boldsymbol{w}} - \hat{p} \nabla \cdot \hat{\boldsymbol{w}} + \frac{1}{\mathrm{Re}} (\nabla \hat{\boldsymbol{u}}^{\mathrm{T}}) \cdot (\nabla \hat{\boldsymbol{w}}^{\mathrm{T}}) \right\} dx \\
&\quad + \int_{\Omega(\boldsymbol{\phi})} \hat{q} \nabla \cdot \hat{\boldsymbol{u}} dx \\
&\quad + h_{\Omega}(\hat{\boldsymbol{u}}, \lambda_r, \tilde{\boldsymbol{u}}_r, \tilde{p}_r, \tilde{\boldsymbol{w}}^{\mathrm{c}}, \tilde{q}^{\mathrm{c}}) + \{ h_{\Omega}(\hat{\boldsymbol{u}}, \lambda_r, \tilde{\boldsymbol{u}}_r, \tilde{p}_r, \tilde{\boldsymbol{w}}^{\mathrm{c}}, \tilde{q}^{\mathrm{c}}) \}^{\mathrm{c}},
\end{aligned}
$$

where

$$
\begin{aligned}
&h_{\Omega}(\hat{\boldsymbol{u}}, \lambda_r, \tilde{\boldsymbol{u}}_r, \tilde{p}_r, \tilde{\boldsymbol{w}}^{\mathrm{c}}, \tilde{q}^{\mathrm{c}}) = \\
&\quad - \int_{\Omega(\boldsymbol{\phi})} \left\{ \lambda_r \tilde{\boldsymbol{u}}_r \cdot \tilde{\boldsymbol{w}}^{\mathrm{c}} + N(\tilde{\boldsymbol{u}}_r, \hat{\boldsymbol{u}}) \cdot \tilde{\boldsymbol{w}}^{\mathrm{c}} - \tilde{p}_r \nabla \cdot \tilde{\boldsymbol{w}}^{\mathrm{c}} \right. \\
&\quad \left. + \frac{1}{\mathrm{Re}} (\nabla \tilde{\boldsymbol{u}}_r^{\mathrm{T}}) \cdot (\nabla \tilde{\boldsymbol{w}}^{\mathrm{c}\mathrm{T}}) \right\} dx \\
&\quad + \int_{\Omega(\boldsymbol{\phi})} \tilde{q}^{\mathrm{c}} \nabla \cdot \tilde{\boldsymbol{u}}_r dx.
\end{aligned}
$$

The shape derivative $L'[\boldsymbol{\psi}]$ of L with respect to arbitrary variation of $(\boldsymbol{\psi}, \hat{\boldsymbol{u}}', \hat{p}', \hat{\boldsymbol{w}}', \hat{q}', \lambda_r', \tilde{\boldsymbol{u}}_r', \tilde{p}_r', \tilde{\boldsymbol{w}}', \tilde{q}') \in D \times (W \times Q)^2 \times \mathbb{C} \times (\tilde{U} \times \tilde{Q})^2$ is obtainable using the formula of (2) as

$$
\begin{aligned}
L'[\boldsymbol{\psi}] &= L_{\boldsymbol{\phi}}[\boldsymbol{\psi}] + L_{\hat{\boldsymbol{u}}, \hat{p}}[\hat{\boldsymbol{u}}', \hat{p}'] + L_{\hat{\boldsymbol{w}}, \hat{q}}[\hat{\boldsymbol{w}}', \hat{q}'] \\
&\quad + 2\mathrm{Real}\Big[L_{\lambda_r}[\lambda_r'] + L_{\tilde{\boldsymbol{u}}_r, \tilde{p}_r}[\tilde{\boldsymbol{u}}_r', \tilde{p}_r'] + L_{\tilde{\boldsymbol{w}}, \tilde{q}}[\tilde{\boldsymbol{w}}', \tilde{q}'] \Big],
\end{aligned}
$$

where

$$
\begin{aligned}
&L_{\boldsymbol{\phi}}[\boldsymbol{\psi}] = \\
&\quad - \int_{\Gamma(\boldsymbol{\phi})} \left\{ \left((\hat{\boldsymbol{u}} \cdot \boldsymbol{\nabla})\, \hat{\boldsymbol{u}} \right) \cdot \hat{\boldsymbol{w}} - \hat{p} \boldsymbol{\nabla} \cdot \hat{\boldsymbol{w}} + \frac{1}{\mathrm{Re}} (\boldsymbol{\nabla} \hat{\boldsymbol{u}}^{\mathrm{T}}) \cdot (\boldsymbol{\nabla} \hat{\boldsymbol{w}}^{\mathrm{T}}) \right\} \boldsymbol{\nu} \cdot \boldsymbol{\psi} d\gamma \\
&\quad + \int_{\Gamma(\boldsymbol{\phi})} (\hat{q} \boldsymbol{\nabla} \cdot \hat{\boldsymbol{u}})\, \boldsymbol{\nu} \cdot \boldsymbol{\psi} d\gamma \\
&\quad + 2\mathrm{Real}\Big[h_{\Gamma_{\mathrm{wall}}}(\hat{\boldsymbol{u}}, \lambda_r, \tilde{\boldsymbol{u}}_r, \tilde{p}_r, \tilde{\boldsymbol{w}}^{\mathrm{c}}, \tilde{q}^{\mathrm{c}}) \Big], \\
&L_{\hat{\boldsymbol{u}}, \hat{p}}[\hat{\boldsymbol{u}}', \hat{p}'] = \\
&\quad - \int_{\Omega(\boldsymbol{\phi})} \{ ((\hat{\boldsymbol{u}}' \cdot \nabla)\, \hat{\boldsymbol{u}}) \cdot \hat{\boldsymbol{w}} + (\hat{\boldsymbol{u}} \cdot \nabla) \hat{\boldsymbol{u}}') \cdot \hat{\boldsymbol{w}} - \hat{p}' \nabla \cdot \hat{\boldsymbol{w}} \\
&\quad + \frac{1}{\mathrm{Re}} (\nabla \hat{\boldsymbol{u}}'^{\mathrm{T}}) \cdot (\nabla \hat{\boldsymbol{w}}^{\mathrm{T}}) \Big\} dx + \int_{\Omega(\boldsymbol{\phi})} \hat{q} \nabla \cdot \hat{\boldsymbol{u}}' dx \\
&\quad - \int_{\Omega(\boldsymbol{\phi})} 2\mathrm{Real}\Big[N(\tilde{\boldsymbol{u}}_r, \hat{\boldsymbol{u}}') \cdot \tilde{\boldsymbol{w}}^{\mathrm{c}} \Big] dx,
\end{aligned}
$$

$$
\begin{aligned}
&L_{\hat{\boldsymbol{w}},\hat{q}}[\hat{\boldsymbol{w}}',\hat{q}'] = \\
&\quad -\int_{\Omega(\boldsymbol{\phi})} \left\{ ((\hat{\boldsymbol{u}}\cdot\nabla)\,\hat{\boldsymbol{u}})\cdot\hat{\boldsymbol{w}}' - \hat{p}\nabla\cdot\hat{\boldsymbol{w}}' + \frac{1}{\mathrm{Re}}(\nabla\hat{\boldsymbol{u}}^{\mathrm{T}})\cdot(\nabla\hat{\boldsymbol{w}}'^{\mathrm{T}}) \right\} dx \\
&\quad +\int_{\Omega(\boldsymbol{\phi})} \hat{q}'\nabla\cdot\hat{\boldsymbol{u}}dx, \\
&L_{\lambda_r}[\lambda_r'] = \lambda_r' - \lambda_r'\int_{\Omega(\boldsymbol{\phi})} \tilde{\boldsymbol{u}}_r\cdot\tilde{\boldsymbol{w}}^{\mathrm{c}}dx, \\
&L_{\tilde{\boldsymbol{u}}_r,\tilde{p}_r}[\tilde{\boldsymbol{u}}_r',\tilde{p}_r'] = h_{\Gamma_{\mathrm{wall}}}(\hat{\boldsymbol{u}},\lambda_r,\tilde{\boldsymbol{u}}_r',\tilde{p}_r',\tilde{\boldsymbol{w}}^{\mathrm{c}},\tilde{q}^{\mathrm{c}}), \\
&L_{\tilde{\boldsymbol{w}},\tilde{q}}[\tilde{\boldsymbol{w}}',\tilde{q}'] = h_{\Gamma_{\mathrm{wall}}}(\hat{\boldsymbol{u}},\lambda_r,\tilde{\boldsymbol{u}}_r,\tilde{p}_r,\tilde{\boldsymbol{w}}'^{\mathrm{c}},\tilde{q}'^{\mathrm{c}}),
\end{aligned}
$$

and

$$
\begin{aligned}
&h_{\Gamma_{\mathrm{wall}}}(\hat{\boldsymbol{u}},\lambda_r,\tilde{\boldsymbol{u}}_r,\tilde{p}_r,\tilde{\boldsymbol{w}}^{\mathrm{c}},\tilde{q}^{\mathrm{c}}) = \\
&\quad -\int_{\Gamma_{\mathrm{wall}}(\boldsymbol{\phi})} \{\lambda_r\tilde{\boldsymbol{u}}_r\cdot\tilde{\boldsymbol{w}}^{\mathrm{c}} + N(\tilde{\boldsymbol{u}}_r,\hat{\boldsymbol{u}})\cdot\tilde{\boldsymbol{w}}^{\mathrm{c}} - \tilde{p}_r\nabla\cdot\tilde{\boldsymbol{w}}^{\mathrm{c}} \\
&\quad +\frac{1}{\mathrm{Re}}(\nabla\tilde{\boldsymbol{u}}_r^{\mathrm{T}})\cdot(\nabla\tilde{\boldsymbol{w}}^{\mathrm{c}\mathrm{T}}) \Big\} d\gamma + \int_{\Gamma_{\mathrm{wall}}(\boldsymbol{\phi})} \tilde{q}^{\mathrm{c}}\nabla\cdot\tilde{\boldsymbol{u}}_r d\gamma.
\end{aligned}
$$

Stationary conditions for $\boldsymbol{\phi}$, $\hat{\boldsymbol{u}}$, $\hat{p}$, $\hat{\boldsymbol{w}}$, $\hat{q}$, λ_r, $\tilde{\boldsymbol{u}}_r$, $\tilde{p}_r$, $\tilde{\boldsymbol{w}}$ and $\tilde{q}$, which are known as the Kuhn–Tucker conditions in optimization theory, are given as

$$
\begin{aligned}
&L_{\hat{\boldsymbol{u}},\hat{p}}[\hat{\boldsymbol{u}}',\hat{p}'] = 0 \quad \forall(\hat{\boldsymbol{u}}',\hat{p}') \in W\times Q, && (23)\\
&L_{\hat{\boldsymbol{w}},\hat{q}}[\hat{\boldsymbol{w}}',\hat{q}'] = 0 \quad \forall(\hat{\boldsymbol{w}}',\hat{q}') \in W\times Q, && (24)\\
&\mathrm{Real}\Big[L_{\lambda_r}[\lambda_r']\Big] = 0 \quad \forall\lambda_r' \in \mathbb{C}, && (25)\\
&\mathrm{Real}\Big[L_{\tilde{\boldsymbol{u}}_r,\tilde{p}_r}[\tilde{\boldsymbol{u}}_r',\tilde{p}_r']\Big] = 0 \quad \forall(\tilde{\boldsymbol{u}}_r',\tilde{p}_r') \in \tilde{U}\times\tilde{Q}, && (26)\\
&\mathrm{Real}\Big[L_{\tilde{\boldsymbol{w}},\tilde{q}}[\tilde{\boldsymbol{w}}',\tilde{q}']\Big] = 0 \quad \forall(\tilde{\boldsymbol{w}}',\tilde{q}') \in \tilde{U}\times\tilde{Q}. && (27)
\end{aligned}
$$

Equations (24) and (27) agree respectively with the weak form of Problem 1 and Problem 2.

Equation (26) is obtained as the weak form of the adjoint equations of Problem 2. Its strong form is written in the following way.

Problem 4 (Adjoint linear disturbance for f) Let $\boldsymbol{\phi}\in D$ and the solution λ_r and $(\tilde{\boldsymbol{u}}_r,\tilde{p}_r)\in\tilde{U}\times\tilde{Q}$ of Problem 2 for r defined in Problem 3 be given. Find $(\tilde{\boldsymbol{w}},\tilde{q}) : \Omega(\boldsymbol{\phi})\to\mathbb{C}^3$ such that

$$
\begin{aligned}
&\mathrm{Real}\Big[\lambda_r\tilde{\boldsymbol{w}}^{\mathrm{c}} + (\nabla\tilde{\boldsymbol{u}}_r^{\mathrm{T}})\hat{\boldsymbol{w}}^{\mathrm{c}} - (\tilde{\boldsymbol{u}}_r\cdot\nabla)\,\hat{\boldsymbol{w}}^{\mathrm{c}} + \nabla\tilde{q}^{\mathrm{c}} - \frac{1}{\mathrm{Re}}\triangle\tilde{\boldsymbol{w}}^{\mathrm{c}}\Big] \\
&\quad = \boldsymbol{0} \quad \text{in } \Omega(\boldsymbol{\phi}), && (28)\\
&\mathrm{Real}\Big[\nabla\cdot\tilde{\boldsymbol{w}}^{\mathrm{c}}\Big] = \boldsymbol{0} \quad \text{in } \Omega(\boldsymbol{\phi}), && (29)\\
&\mathrm{Real}\Big[\frac{1}{\mathrm{Re}}(\boldsymbol{\nabla}\tilde{\boldsymbol{w}}^{\mathrm{c}\mathrm{T}})\boldsymbol{\nu} - \tilde{q}^{\mathrm{c}}\boldsymbol{\nu}\Big] = \boldsymbol{0} \quad \text{on } \Gamma_{\mathrm{out}\,0} && (30)
\end{aligned}
$$

$$\tilde{\boldsymbol{w}} = \boldsymbol{0} \text{ on } \Gamma_{\text{in}\,0} \cup \Gamma_{\text{wall}}(\boldsymbol{\phi}), \tag{31}$$

$$\text{Real}\left[\int_{\Omega(\boldsymbol{\phi})} \tilde{\boldsymbol{u}}_r \cdot \tilde{\boldsymbol{w}}^{\text{c}} dx\right] = -1 \tag{32}$$

Moreover, (23) is obtained as the weak form of the adjoint equations of Problem 1. Its strong form is expressed in the following way.

Problem 5 (Adjoint stationary Navier–Stokes for f) For $\boldsymbol{\phi} \in D$ and the soultions $(\hat{\boldsymbol{u}}, \hat{p}) \in U \times Q$ of Problem 3 and $(\tilde{\boldsymbol{w}}, \tilde{q}) \in \tilde{U} \times \tilde{Q}$ of Problem 2. Find $(\hat{\boldsymbol{w}}, \hat{q}) : \Omega(\boldsymbol{\phi}) \to \mathbb{R}^3$ such that

$$\begin{aligned}&(\nabla \hat{\boldsymbol{u}}^{\text{T}})\hat{\boldsymbol{w}} - (\hat{\boldsymbol{u}} \cdot \nabla)\,\hat{\boldsymbol{w}} + 2\text{Real}\Big[(\nabla \tilde{\boldsymbol{u}}_r^{\text{T}})\tilde{\boldsymbol{w}}^{\text{c}} - (\tilde{\boldsymbol{u}}_r \cdot \nabla)\,\tilde{\boldsymbol{w}}^{\text{c}}\Big] \\ &\quad = -\nabla \hat{q} + \frac{1}{\text{Re}} \triangle \hat{\boldsymbol{u}} \quad \text{in } \Omega(\boldsymbol{\phi}),\end{aligned} \tag{33}$$

$$\nabla \cdot \hat{\boldsymbol{w}} = 0 \quad \text{in } \Omega(\boldsymbol{\phi}), \tag{34}$$

$$\frac{1}{\text{Re}}(\boldsymbol{\nabla} \hat{\boldsymbol{w}}^{\text{T}})\boldsymbol{\nu} - \hat{p}\boldsymbol{\nu} = \boldsymbol{0} \quad \text{on } \Gamma_{\text{out}\,0} \tag{35}$$

$$\hat{\boldsymbol{w}} = \boldsymbol{0} \quad \text{on } \Gamma_{\text{in}\,0} \cup \Gamma_{\text{wall}}(\boldsymbol{\phi}). \tag{36}$$

Here, using the solutions $(\hat{\boldsymbol{u}}, \hat{p})$ and $(\hat{\boldsymbol{w}}, \hat{q})$ of Problem 1 and Problem 5, respectively, and the solutions $(\lambda_r, \tilde{\boldsymbol{u}}_r, \tilde{p}_r)$ and $(\tilde{\boldsymbol{w}}, \tilde{q})$ of Problem 2 and Problem 4, respectively, we have

$$L'[\boldsymbol{\psi}] = L_{\boldsymbol{\phi}}[\boldsymbol{\psi}] = \int_{\Gamma(\boldsymbol{\phi})} G\boldsymbol{\nu} \cdot \boldsymbol{\psi} dx, \tag{37}$$

where $G\boldsymbol{\nu}$ is called the shape gradient of f, and G is given as

$$G = -\frac{1}{\text{Re}}(\nabla \hat{\boldsymbol{u}}^{\text{T}}) \cdot (\nabla \hat{\boldsymbol{w}}^{\text{T}}) - 2\text{Real}\Big[\frac{1}{\text{Re}}(\nabla \tilde{\boldsymbol{u}}_r^{\text{T}}) \cdot (\nabla \tilde{\boldsymbol{w}}^{\text{cT}})\Big].$$

4 Numerical scheme

The H^1 gradient method becomes applicable to obtain the variation of a design variable that decreases the cost function [2] if the shape gradient of cost function is evaluated. The H^1 gradient method was proposed as a procedure for solving the variation of the design variable as a solution of a boundary value problem of elliptic partial differential equation assuming that the linear form of a given function in the weak form of the boundary value problem is replaced by the Fréchet derivative with a negative sign. For these analyses, we use the weak form of the method in the following way. Find $\boldsymbol{\psi} \in X$ satisfying

$$c_a \int_{\Omega(\boldsymbol{\phi})} \boldsymbol{E}(\boldsymbol{\psi}) \cdot \boldsymbol{E}(\boldsymbol{y}) dx = -\int_{\Gamma(\boldsymbol{\phi})} G\boldsymbol{\nu} \cdot \boldsymbol{y} d\gamma, \tag{38}$$

for all $\boldsymbol{y} \in X$. Here, c_a is a positive constant to control the magnitude of $\boldsymbol{\psi}$ and $\boldsymbol{E}(\boldsymbol{u})$ is the strain tensor:

$$\boldsymbol{E}(\boldsymbol{u}) = \frac{1}{2}\left(\boldsymbol{\nabla}\boldsymbol{u}^{\mathrm{T}} + (\boldsymbol{\nabla}\boldsymbol{u}^{\mathrm{T}})^{\mathrm{T}}\right).$$

Since X is defined by (1), the strong form of the boundary value problem is written in the following way.

Problem 6 (H^1 gradient method of domain variation type) For $\boldsymbol{\phi} \in D$, let $G\boldsymbol{\nu}$ in (37) be given. Find $\boldsymbol{\psi} \in X$ such that

$$\begin{aligned} &- c_a \boldsymbol{\nabla}^{\mathrm{T}} \boldsymbol{E}(\boldsymbol{\psi}) = \boldsymbol{0}^{\mathrm{T}} \quad \text{in } \Omega(\boldsymbol{\phi}), \\ &c_a \boldsymbol{E}(\boldsymbol{\psi})\boldsymbol{\nu} = -G\boldsymbol{\nu} \quad \text{on } \Gamma_{\mathrm{wall}}(\boldsymbol{\phi}), \\ &\boldsymbol{\psi} = \boldsymbol{0} \quad \text{on } \Gamma_{\mathrm{in}\,0} \cup \Gamma_{\mathrm{out}\,0}. \end{aligned}$$

The scheme to solve Problem 3 is described as presented below.

(1) Set Ω_0, $\Gamma_{\mathrm{wall}\,0}$ and c_a in (38), and put $k = 0$.
(2) Solve Problem 1 and Problem 2, and compute f in (22).
(3) Solve Problem 4 and Problem 5, and compute $-G\boldsymbol{\nu}$ in (37).
(4) Solve $\boldsymbol{\psi}$ in Problem 6.
(5) Reshape $\Omega(\boldsymbol{\phi})$ by $\Omega(\boldsymbol{\phi} + \boldsymbol{\psi})$, and do (2).
(6) Judge convergence.
  – If the terminal condition is satisfied, then proceed to (7).
  – Otherwise, replace $k + 1$ with k and return to (3).
(7) Stop iteration.

In the scheme above, the following methods based on the finite element method are used. Problem 1 and Problem 2 are solved respectively by the Newton method and the Arnoldi method. Problem 4 and Problem 5 are solved, respectively, by the Newton method and UMFPACK[10]. Problem 6 is solved by UMFPACK[10].

5 Numerical results

Validity of our method is demonstrated by a numerical example about the two-dimensional Poiseulle flow in a channel with a sudden expansion. We use the initial domain Ω_0 and the boundaries of $\Gamma_{\mathrm{in}\,0}$, $\Gamma_{\mathrm{out}\,0}$ and $\Gamma_{\mathrm{wall}\,0}$ as shown in Section 2. On $\Gamma_{\mathrm{in}\,0}$, the Poiseuille flow is assumed as $\hat{u}_{\mathrm{D}} = 1 - y^2$ and $\hat{v}_{\mathrm{D}} = 0$. For the domain variation, $\Gamma_{\mathrm{in}\,0} \cup \Gamma_{\mathrm{out}\,0}$ is fixed as defined in (1).

For finite element analyses, the P2/P1 element for the velocity and the pressure is used to discretize equations spatially. Figure 1 shows finite element meshes of the initial domain. The numbers of nodes and elements are, respectively, 15268 and 7935.

For the scheme presented above, we use $c_a = 10^{-7}$ and $|f_{k+1} - f_k| < 10^{-4}$ as the terminal condition for the iteration number k. In this study, referring to the

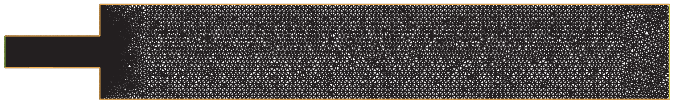

(a) Whole view

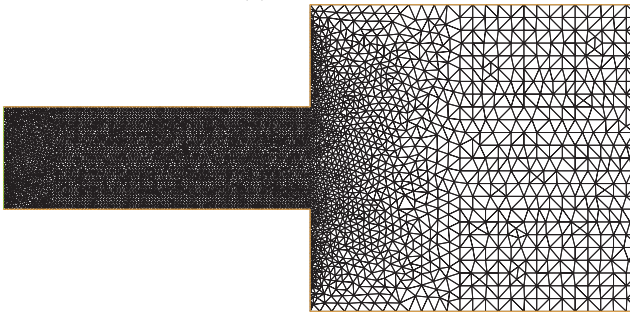

(b) Zoomed view

Fig. 1 Finite element mesh of initial domain Ω_0.

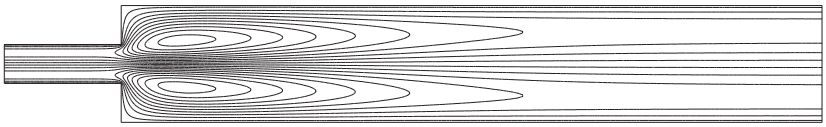

Fig. 2 Stream function $\hat{\psi}$ in initial domain Ω_0 at $\mathrm{Re} = 45$.

report of $\mathrm{Re_c} = 40.24$ by Mizushima and Shiotani [23], the two main problems and the shape optimization problems are demonstrated at $\mathrm{Re} = 45$. Figure 2 shows the contours of the stream function $\hat{\psi}$ for the initial domain, where the velocity $(\hat{u}, \hat{v})$ is defined with $\hat{\psi}$ by $\left(\partial\hat{\psi}/\partial y, -\partial\hat{\psi}/\partial x\right)$. For the mode number r used in Problem 3, $r = 1$ is used in which the mode numbers are defined in descending order of the magnitude of the real parts of the eigenvalues.

The domain optimized by the present scheme is presented in Fig. 3. Figure 4 shows the flow field in the optimized domain. The iteration history of the cost function $f = 2\mathrm{Real}[\lambda_1]$ with respect to reshaping is presented in Fig. 5. Figure 6 shows the iteration history of $\mathrm{Imag}[\lambda_1]$. The graphs of the real part of λ_1 with respect to the Reynolds number are presented in Fig. 8. Distributions of λ_i at $\mathrm{Re} = 45$ are shown in Fig. 7. Table 1 depicts the eigenvalue $\lambda_1, \cdots, \lambda_5$ on initial domain Ω_0 and the optimized domain $\Omega(\boldsymbol{\phi})$ at $\mathrm{Re} = 45$.

Comparing Fig. 3 with Fig. 1 shows that the part of $0 \leq x \leq 6$ bends upward by shape optimization. By this change, it is considered that the lower vortex becomes dominant as observed in comparison of Figs. 2 and 4, and that the flow field is stabilized. From Figs. 5 and 6, the real part of λ_1 decreases from a positive value to a negative value in the reshaping iterations, while the imaginary part of λ_1 remains 0 after the real part becomes negative. Figure 8 shows in a straightforward manner that the critical Reynolds number increased

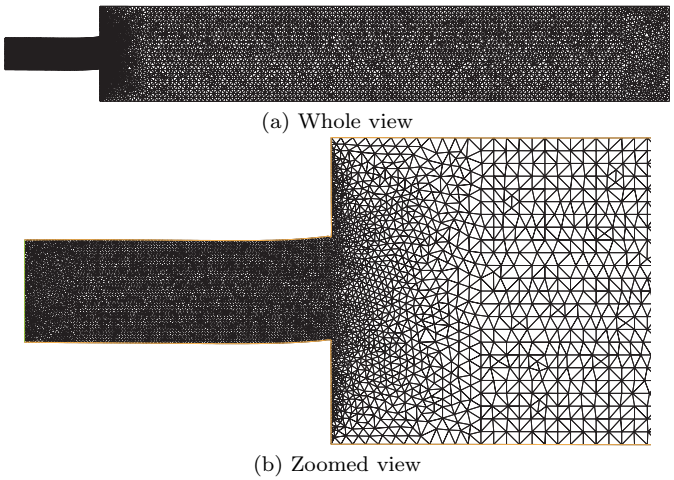

(a) Whole view

(b) Zoomed view

Fig. 3 Finite element mesh of optimized domain $\Omega(\boldsymbol{\phi})$.

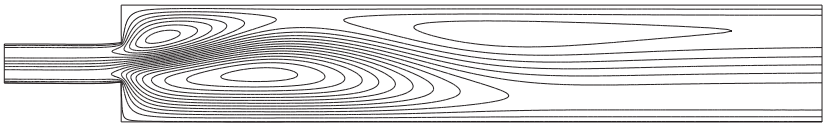

Fig. 4 Stream function $\hat{\psi}$ in optimized domain $\Omega(\boldsymbol{\phi})$ at Re = 45.

Table 1 Eigenvalues $\lambda_1, \cdots, \lambda_5$ on initial domain Ω_0 and optimized domain $\Omega(\boldsymbol{\phi})$ at Re = 45.

λ_i	Initial domain	Optimal domain
λ_1	(0.00332525, 0)	(-0.000232143, 0)
λ_2	(0.00120482, 0)	(-0.016787, 0)
λ_3	(-0.0417513, 0)	(-0.0405093, 0)
λ_4	(-0.0610598, 0)	(-0.0624071, $\pm$0.0496655)
λ_5	(-0.0652305, $\pm$0.0532776)	(-0.0706416, 0)

from 40.24 at the initial domain to 45.49 at the optimized domain by the optimization process. This result of the initial shape accords with the result by Mizushima and Shiotani [23], who reported that a steady state solution appears after Re passes 40.24 on the two-dimensional Poiseuille flow with a sudden expansion. However, the critical Reynolds number of the final shape obtained by our method is bigger than that.

6 Summary

In this paper, we formulated a shape optimization problem of flow field for delaying the transition from laminar flow to turbulent flow, and presented

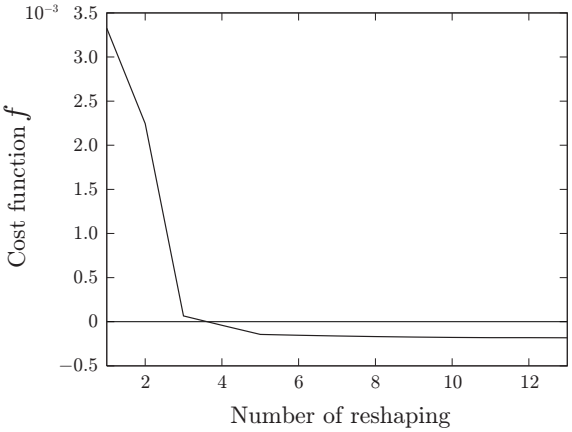

Fig. 5 Iteration history of $f = 2\mathrm{Real}[\lambda_1]$ at $\mathrm{Re} = 45$.

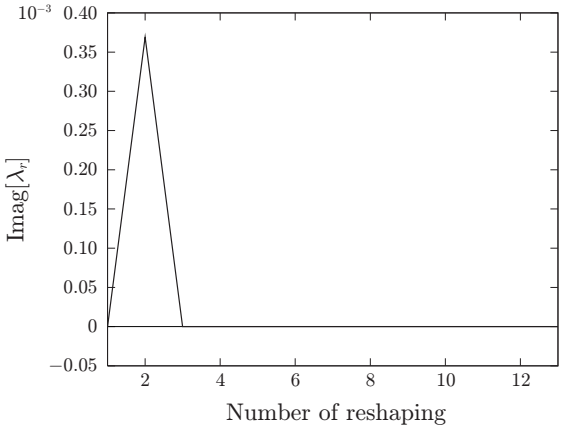

Fig. 6 Iteration history of imaginary part of λ_1 at $\mathrm{Re} = 45$.

the solution of the problem based on the gradient based method. In the formulation, mapping from an initial domain to a new domain was chosen as a design variable. For a given domain, the main problems were defined by the stationary Navier–Stokes problem and an eigenvalue problem assuming a linear disturbance in the solution of the stationary Navier–Stokes problem. An objective cost function was defined by the maximum value of the real part of the eigenvalues. The shape derivative of the cost function was evaluated by the Lagrange multiplier method. For numerical scheme, we use an iterative algorithm based on the H^1 gradient method using the finite element method. A numerical analysis for two-dimensional Poiseuille flow with sudden expansion was conducted to confirm the validity of the scheme. Results revealed that a critical Reynolds number increases by the iteration of reshaping.

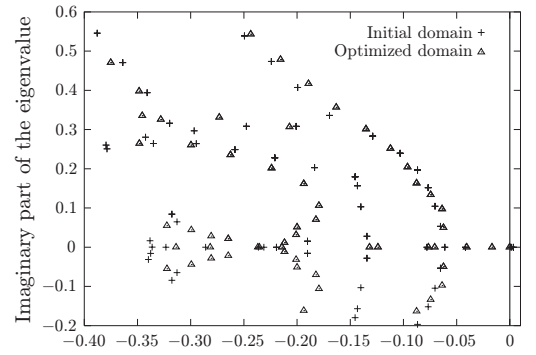

(a) Wide view

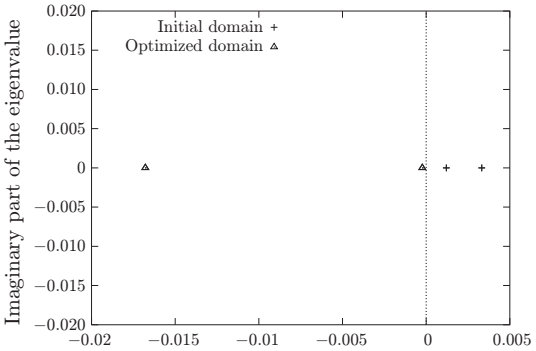

(b) Zoomed view

Fig. 7 Distributions of λ_i at Re = 45.

References

1. Azegami, H.: A solution to domain optimization problems (in Japanese). Trans. of Jpn. Soc. of Mech. Engs., Ser. A **60**(574), 1479–1486 (1994)
2. Azegami, H.: Regularized solution to shape optimization problem (in Japanese). Trans. of Jpn. Soc. for Indust. Appl. Math. **23**(2), 83–138 (2014)
3. Azegami, H., Fukumoto, S., Aoyama, T.: Shape optimization of continua using NURBS as basis functions. Struct. and Multidiscip. Opt. **47**(2), 247–258 (2013).Structural and Multidisciplinary Optimization DOI 10.1007/s00158-012-0822-4
4. Azegami, H., Kaizu, S., Takeuchi, K.: Regular solution to topology optimization problems of continua. JSIAM Letters **3**, 1–4 (2011)
5. Azegami, H., Takeuchi, K.: A smoothing method for shape optimization: Traction method using the Robin condition. Int. J. of Compt. Methods **3**(1), 21–33 (2006)
6. Azegami, H., Wu, Z.Q.: Domain optimization analysis in linear elastic problems: Approach using traction method. JSME Int. J., Ser. A **39**(2), 272–278 (1996)
7. Belson, A.B., Semeraro, O., Rowley, C.W., Henningson, S.D.: Feedback control of instabilities in the two-dimensional Blasius boundary layer: The role of sensors and actuators. Phys. Fluids **25**(054106) (2013). DOI 10.1063/1.4804390
8. Camarri, S., Iollo, A.: Feedback control of the vortex-shedding instability based on sensitivity analysis. Phys. Fluids **22**(094102) (2010). DOI 10.1063/1.3481148

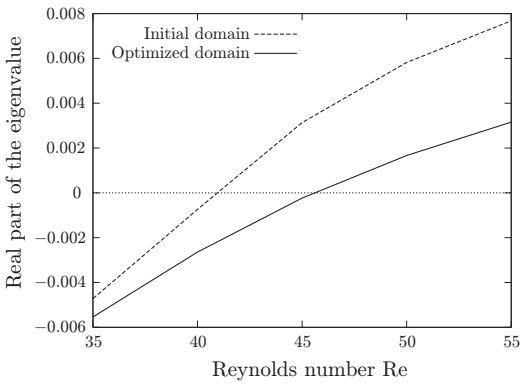

Fig. 8 Real part of λ_1 with respect to the Reynolds number.

9. Chenais, D.: On the existence of a solution in a domain identification problem. J. Math. Anal. Appl. **52**, 189–219 (1975)
10. Davis, T.: Algorithm 832: UMFPACK, an unsymmetric-pattern multifrontal method. ACM Trans. on Math. Software. **30**, 196–199 (2004)
11. Fani, A., Camarri, S., Salvetti, V.M.: Stability analysis and control of the flow in a symmetric channel with a sudden expansion. Phys. Fluids **24**(084102) (2012). DOI 10.1063/1.4745190
12. Glowinski, R., Pironneau, O.: On the numerical computation of minimum-drag profile in laminar flow. J. Fluid. Mech. **72**(2), 385–389 (1975)
13. Hadamard, J.: Mémoire des savants etragers. Oeuvres de J. Hadamard, chap. Mémoire sur le probléme d'analyse relatif á l'équilibre des plaques élastiques encastrées, Mémoire des savants etragers, Oeuvres de J. Hadamard, pp. 515–629. CNRS, Paris (1968)
14. Haslinger, J., Mäkinen, R.A.E.: Introduction to Shape Optimization: Theory, Approximation, and Computation. SIAM, Philadelphia (2003)
15. Haslinger, J., Málek, J., Stebel, J.: Shape optimization in problems governed by generalised Navier-Stokes equations: existence analysis. Control and Cybern. **34**(1), 283–303 (2005)
16. Huan, J., Modi, V.: Optimum design of minimum drag bodies in incompressible laminar flow using a control theory approach. Inverse Problems in Eng. **1**(1), 1–25 (1994)
17. Huan, J., Modi, V.: Design of minimum drag bodies in incompressible laminar flow. Inverse Problems in Eng. **3**(1), 233–260 (1996)
18. Imam, M.H.: Three-dimensional shape optimization. Int. J. Num. Meth. Engrg. **18**, 661–673 (1982)
19. Kaizu, S.: The Gateau derivative of cost functions in the optimal shape problems and the existence of the shape derivatives of solutions of the Stokes problems. JSIAM Letters **1**, 17–20 (2009)
20. Katamine, E., Azegami, H., Tsubata, T., Itoh, S.: Solution to shape optimization problems of viscous flow fields. Int. J. of Comput. Fluid Dynamics **19**(1), 45–51 (2005)
21. Katamine, E., Nagatomo, Y., Azegami, H.: Shape optimization of 3d viscous flow fields. Inverse Problems of Sci. Eng. **17**(1), 105–114 (2009)
22. Marquet, O., Sipp, D., Jacquin, L.: Sensitivity analysis and passive control of cylinder flow. J. Fluid. Mech. **615**, 221–252 (2008)
23. Mizushima, J., Shiotani, Y.: Structural instability of the bifurcation diagram for two-dimensional flow in a channel with a sudden expansion. Comput. Methods Appl. Mech. Engrg. **420**, 131–145 (2000)
24. Mohammadi, B., Pironneau, O.: Applied shape optimization for fluids. Oxford University Press, Oxford, New York (2001)
25. Pironneau, O.: On optimum profiles in Stokes flow. J. Fluid. Mech. **59**(1), 117–128 (1973)

26. Pironneau, O.: On optimum design in fluid mechanics. J. Fluid. Mech. **64**(1), 97–110 (1974)
27. Pironneau, O.: Optimal Shape Design for Elliptic Systems. Springer-Verlag, New York (1984)
28. Sano, M., Sakai, H.: Numerical determination of minimum drag profile in Stokes flow (in case of two-dimensional finite region and constant cross-sectional area). Trans. Jpn. Soc. Aeronaut. Space Sci. **26**(71), 1–9 (1983)
29. Shapira, M., Degani, D., Weihs, D.: Stability and existence of multiple solutions for viscous flow in suddenly enlarged channels. Computations and Fluids **18**, 239–258 (1990)
30. Sipp, D., Marquet, O., Meliga, P., Barbagallo, A.: Dynamics and control of global instabilities in open flows: a linearized approach. Appl. Mech. Rev. **63**(030801), 1–26 (2010). DOI 10.1115/1.4001478
31. Sokolowski, J., Zolésio, J.P.: Introduction to Shape Optimization: Shape Sensitivity Analysis. Springer-Verlag, New York (1992)